Preprints.org

Article

Not peer-reviewed version

Mutual Information and Quantum Coherence in Minimum Error Discrimination of N Pure Equidistant Quantum States

Omar Jiménez *

Posted Date: 25 June 2025

doi: 10.20944/preprints202506.1981.v1

Keywords: mutual information; quantum coherence; quantum state discrimination; equidistant states

Preprints.org is a free multidisciplinary platform providing preprint service that is dedicated to making early versions of research outputs permanently available and citable. Preprints posted at Preprints.org appear in Web of Science, Crossref, Google Scholar, Scilit, Europe PMC.

Copyright: This open access article is published under a Creative Commons CC BY 4.0 license, which permit the free download, distribution, and reuse, provided that the author and preprint are cited in any reuse.

Preprints.org (www.preprints.org) | NOT PEER-REVIEWED | Posted: 25 June 2025 doi:10.20944/preprints202506.1981.v1

Disclaimer/Publisher's Note: The statements, opinions, and data contained in all publications are solely those of the individual author(s) and contributor(s) and not of MDPI and/or the editor(s). MDPI and/or the editor(s) disclaim responsibility for any injury to people or property resulting from any ideas, methods, instructions, or products referred to in the content.

Article

Mutual Information and Quantum Coherence in Minimum Error Discrimination of N Pure Equidistant Quantum States

Omar Jiménez

Centro Multidisciplinario de Física, Vicerrectoría de Investigación, Universidad Mayor, 8580745 Santiago, Chile; omar.jimenez@umayor.cl

Abstract

We study the quantum state discrimination problem under the minimum error (ME) strategy for a set of N pure equidistant states. These states are characterized by the property that the inner product between any pair of states is given by a unique complex number S. We provide the explicit form of the states and analyze their main structural properties. The optimal success probability for ME discrimination is evaluated as a function of the number of states, as well as the modulus and phase of the inner product S. Furthermore, we propose an experimental scheme for implementing the ME discrimination of equidistant states. We also investigate the quantum coherence consumed in the implementation of the minimum error discrimination of the equidistant states, which has an established operational interpretation as cryptographic randomness gain. As an application, we propose a quantum communication protocol in which Alice prepares and sends one of the equidistant states, while Bob applies the minimum error discrimination to extract the classical information encoded in the state. Finally, we discuss the optimal conditions under which the protocol achieves an optimal balance of classical correlations and quantum coherence, thereby ensuring effective information transfer and cryptographic security.

Keywords: mutual information; quantum coherence; quantum state discrimination; equidistant states

1. Introduction

One of the main applications of quantum information theory is the development of quantum communication protocols [1,2]. In such protocols, two legitimate parties, commonly referred to as Alice and Bob, aim to share information securely. Meanwhile, an adversary, known as Eve, attempts to intercept the information without being detected. To establish communication, Alice and Bob agree on a set of quantum states, which are typically chosen to be nonorthogonal. A key property of nonorthogonal quantum states is that they cannot be perfectly distinguishability by any quantum measurement [3,4]. This inherent indistinguishability underlies the security of quantum communication protocols, such as the well-known BB84 scheme [5]. In a typical communication protocol, Alice prepares and transmits classical information encoded in a set of nonorthogonal quantum states. At the distant end of the communication channel, Bob receives the quantum state and performs a measurement to extract the information sent by Alice. The specific quantum measurement employed by Bob is chosen to optimize a predefined figure of merit. For example, he may implement a measurement that minimizes the probability of error in identifying the transmitted states (ME) [6–8] or one that allows the extraction of the accessible information (MI) [9–11], which quantifies the maximal classical correlation that can be established between the legitimate parties. In general, these correspond to two distinct optimization problems [12]. However, when the set consists of two pure nonorthogonal states prepared with arbitrary *a priori* probabilities, it is known that ME and MI measurements coincide [4,11–15]. The optimization problem consists of finding the optimal set of quantum measurement

© 2025 by the author(s). Distributed under a Creative Commons CC BY license.

Preprints.org (www.preprints.org) | NOT PEER-REVIEWED | Posted: 25 June 2025 doi:10.20944/preprints202506.1981.v1

operators. For minimum error discrimination, the necessary and sufficient conditions that the optimal measurement operators must satisfy are well establish [6,7]. In contrast, for the accessible information only necessary condition are known [6,16,17]. Analytical solutions for the ME strategy are available for specific classes of quantum states [6–8,17–21]. On the other hand, the MI optimization problem is significantly more challenging, and exact solutions are known only for a few cases [22–24]. Nevertheless, there exists lower and upper bounds for the accessible information [16,25,26], and several results have been reported regarding the number of measurement operators required to implement the MI strategy [10,11]. Minimum error discrimination plays a key role in various quantum information processing tasks, including quantum teleportation [27,28], entanglement swapping [29,30], quantum cryptography [31] and dense coding [32], among others. Furthermore, the ME of nonorthogonal states has been successfully demonstrated in several experimentally settings [12,33–35]. On the other hand, the accessible information strategy finds application in quantum cryptography [16], and its experimental implementation has been reported in specific scenarios [12].

In this work, we study the minimum error discrimination of a set of N pure, nonorthogonal equidistant quantum states, each prepared with equal *a priori* probability. We derive the optimum measurement operators and the corresponding success probability for ME, and we also propose an experimental scheme for its implementation. Moreover, we evaluate the quantum coherence, involved in applying the ME strategy to the equidistant states, which has the operational interpretation as a cryptographic randomness gain. We then determine the classical correlations shared between Alice and Bob when the ME strategy is employed. Finally, we study the relationship between classical correlations and quantum coherence within the ME protocol. Interestingly, our results reveal a fundamental trade-off: greater classical information sharing between Alice and Bob corresponds to reduced randomness generation, and vice versa.

This article is organized as follows: In Section 2, we introduce and describe the set of N pure, nonorthogonal equidistant quantum states. In Section 3, we derive the optimal measurement operators and the corresponding success probability for the minimum error discrimination of these states, together with a proposal for their experimental implementation. In Section 4, we focuses on the analysis of quantum coherence of the set of equidistant states. In Section 5, We describe the initial and final global states of the composite system shared by Alice and Bob, resulting from the minimum error (ME) measurement performed by Bob. In Section 6, we study the classical correlations shared between Alice and Bob when ME is implemented by Bob. Moreover, we examine the trade-off between Bob's information gain and the quantum coherence consumed in the process. Finally, in Section 7, we summarize our findings and present concluding remarks.

2. Equidistant States

Let us consider a set of N pure, nonorthogonal quantum states denoted by $\{|\psi_j\rangle\}$ with $j = 0, ..., N-1$, satisfying the following property:

$$\langle\psi_j|\psi_{j'}\rangle = S = |S|e^{i\theta}, \qquad \forall\, j > j', \tag{1}$$

that is, the inner product between any two states in the set depends solely on a single complex number S or equivalently, on two real parameters: its modulus $|S|$ and its phase θ. Due to this property, the set is referred to as equidistant [36–38]. For such a set states, the modulus $|S|$ is constrained to lie within the interval $|S| \in [0, |S_\theta|]$, where $|S_\theta|$ is a function of the phase θ and the number N of states in the set, given by

$$|S_\theta| = \frac{\sin\left(\frac{\pi-\theta}{N}\right)}{\sin\left(\theta + \frac{\pi-\theta}{N}\right)}. \tag{2}$$

© 2025 by the author(s). Distributed under a Creative Commons CC BY license.

Preprints.org (www.preprints.org) | NOT PEER-REVIEWED | Posted: 25 June 2025 doi:10.20944/preprints202506.1981.v1

The explicit form of the set of N pure, nonorthogonal equidistant states is given in [37] as:

$$|\psi_j\rangle = \sum_{k=0}^{N-1} C_k \omega_k^j |k\rangle, \qquad \text{for } j = 0, 1, ..., N-1, \tag{3}$$

where N is fixed, and all the real coefficients C_k in Equation (3) depend only on the modulus $|S|$ and the phase θ of the inner product S. These coefficients are given by

$$C_k = \sqrt{\frac{1}{N}\left[1 - |S| \frac{\sin\left(\theta + \frac{k\pi-\theta}{N}\right)}{\sin\left(\frac{k\pi-\theta}{N}\right)}\right]}, \qquad \text{for } k = 0, 1, ..., N-1. \tag{4}$$

Given the symmetry of the equidistant states, as illustrated in Figure 2, we restrict the phase θ of the inner product S to the interval $[0, \pi]$. Within this interval, the coefficients exhibit an ordering property, namely

$$C_1 \leq C_2 \leq C_3 \leq ... \leq C_0, \tag{5}$$

and the phases ω_k in Equation (3) are defined as

$$\omega_k = e^{\frac{2i}{N}(k\pi-\theta)}, \qquad \text{for } k = 0, 1, ..., N-1. \tag{6}$$

Figure 1 illustrates the ordering of the coefficients C_k, as defined in Equation (5), as a function of $|S|$, for: (a) $N = 3$, (b) $N = 4$, and (c) $N = 5$, with $\theta = \pi/36$. As shown in all cases, the maximum and minimum values of the coefficients correspond to C_0 and C_1, respectively. Moreover, when the states are orthogonal, $|S| = 0$, all coefficients become equal and take the value $1/\sqrt{N}$, where N is the number of states in the set.

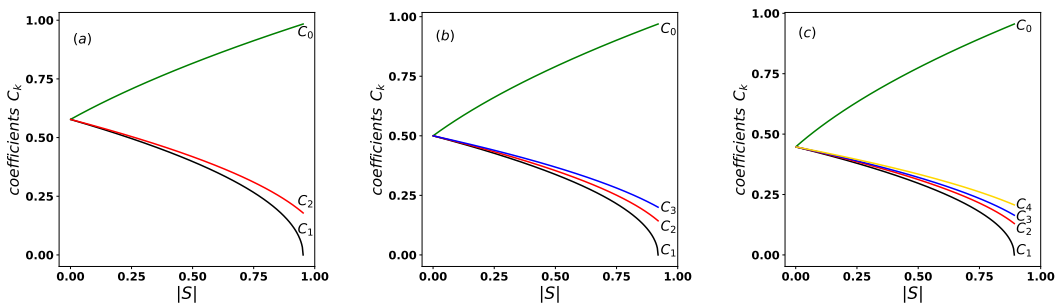

Figure 1. Ordering property of the coefficients C_k from Equation (5) as a function of $|S|$, shown for: (a) $N = 3$, (b) $N = 4$, and (c) $N = 5$, with $\theta = \pi/36$.

Given the coefficients C_k defined in Equation (4), the equidistant states in Equation (3) are properly normalized, that is,

$$\sum_{k=0}^{N-1} C_k^2 = 1. \tag{7}$$

Figure 2 shows, in polar coordinates, the possible values of the inner product S for sets of pure equidistant states, with: a) N=3, b) N=7 and c) N=15. For a given phase θ, the modulus of the inner product S is constrained to lie within the interval $|S| \in [0, |S_\theta|]$. The blue line in Figure 2 corresponds to the case $|S| = |S_\theta|$, for which the set of equidistant states becomes linearly dependent. For instance, when $\theta = 0$, the condition $|S| = |S_\theta| = 1$ implies that all N states are all identical to $|0\rangle$. In this case, the states span a one-dimensional Hilbert space and are therefore linearly dependent. For any other value of θ, the condition $|S| = |S_\theta|$ defines a set of N equidistant states that are linearly dependent and span an $(N-1)-$dimensional Hilbert space. On the other hand, the set of pure equidistant states is linearly independent when the modulus of the inner product lies within the region bounded by the blue line, i.e., for $|S| \in [0, |S_\theta|)$. In this case, the states span an N-dimensional Hilbert space. Figure

© 2025 by the author(s). Distributed under a Creative Commons CC BY license.

Preprints.org (www.preprints.org) | NOT PEER-REVIEWED | Posted: 25 June 2025 doi:10.20944/preprints202506.1981.v1

2 illustrate how the range of possible values for $|S|$ decreases as the the number of states N increase. This implies that, as N increases, the phase θ of the inner product becomes progressively less relevant, ultimately leaving only the case $\theta = 0$ in the limit of large N.

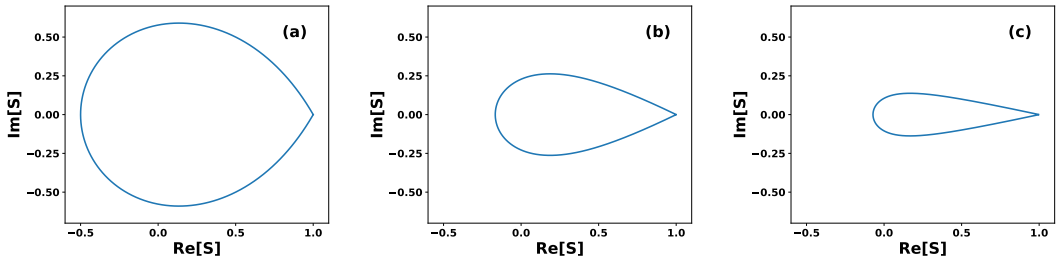

Figure 2. Polar graph of the inner product S. The blue line indicates the boundary $|S| = |S_\theta|$, where the set of equidistant states becomes linearly dependent. Each point inside the bounded region corresponds to a specific value of S and represents a set of N linearly independent equidistant states: (a) N=3, (b) N=7 and (c) N=15.

Another important property of the set of equidistant states is that there exist a unitary transformation U that generates the entire set from a single state, namely

$$|\psi_j\rangle = U^j|\psi_0\rangle, \qquad \text{with } j = 1, 2, ..., N-1, \tag{8}$$

where

$$U = \sum_{k=0}^{N-1} \omega_k |k\rangle\langle k|, \tag{9}$$

with ω_k defined in Equation (6), and $|\psi_0\rangle$ is referred to as the fiducial state. Applying the unitary transformation N times yields

$$U^N = \sum_{k=0}^{N-1} \omega_k^N |k\rangle\langle k| = \sum_{k=0}^{N-1} e^{2i(k\pi-\theta)}|k\rangle\langle k| = e^{-2\theta i}\mathbf{1}_N. \tag{10}$$

Under the condition $U^N = \mathbf{1}_N$, the set of equidistant states is also symmetric. This occurs when $\theta = 0$ or $\theta = \pi$. In the following, we provide a more detailed description of these two particular sets of states.

For $\theta = 0$, the inner product is a real and positive number, with $S = |S|$ and $|S| \in [0, 1]$. In this case, the fiducial state takes the form

$$|\psi_0\rangle = C_0|0\rangle + C_1 \sum_{k=1}^{N-1} |k\rangle, \tag{11}$$

where the coefficients are given by $C_1 = \sqrt{(1-|S|)/N}$ and $C_0 = \sqrt{C_1^2 + |S|}$. The set of N equidistant states is linearly independent (dependent), and spans a N-dimensional(1-dimensional) Hilbert space, if $|S| \in [0, 1)$ ($|S| = 1$), respectively.

For $\theta = \pi$, the inner product is a real and negative, with $S = -|S|$ and $|S| \in [0, \frac{1}{N-1}]$. The fiducial state in this case takes the form

$$|\psi_0\rangle = C_1|1\rangle + C_0 \sum_{k=0,k\neq 1}^{N-1} |k\rangle, \tag{12}$$

with coefficients $C_1 = \sqrt{(1-(N-1)|S|)/N}$ and $C_0 = \sqrt{C_1^2 + |S|}$. Here, the set of N equidistant states is linearly independent (dependent), and spans an N-dimensional (N-1 dimensional) Hilbert space, if $|S| \in [0, \frac{1}{N-1})$ ($|S| = \frac{1}{N-1}$), respectively.

© 2025 by the author(s). Distributed under a Creative Commons CC BY license.

Preprints.org (www.preprints.org) | NOT PEER-REVIEWED | Posted: 25 June 2025 doi:10.20944/preprints202506.1981.v1

3. Minimum Error Discrimination

Having defined the set of N pure nonorthogonal equidistant states $\{|\psi_j\rangle\}_{j=0}^{N-1}$ in [36] and described it in detail in [38], we now study its quantum state discrimination under the minimum error strategy. To this end, we assume that each state $|\psi_j\rangle$ is prepared with equal *a priori* probability, i.e., $\eta_j = 1/N$ for $j = 0, 1, ..., N-1$.

In general, the necessary and sufficient conditions for optimum discrimination with minimum error among N density matrices ρ_k, each prepared with arbitrary *a priori* probabilities η_k, were found by Holevo [6] and Yuen [7]. These conditions are given by

$$\Pi_k(\eta_k\rho_k - \eta_j\rho_j)\Pi_j = 0, \qquad \forall\, j,k, \tag{13}$$

$$(\sum_k \eta_k\Pi_k\rho_k) - \eta_j\rho_j \geq 0, \qquad \forall\, j, \tag{14}$$

where Π_k are the detection operators to be determined for the optimum discrimination of the state ρ_k. In the particular case of a set of N pure nonorthogonal equidistant states prepared with equal *a priori* probability, the above conditions are satisfied when the detection operators are given by

$$\Pi_k = |u_k\rangle\langle u_k|, \qquad \text{for } k = 0, 1, ..., N-1, \tag{15}$$

where the states $|u_k\rangle$ are defined as

$$|u_k\rangle = \frac{1}{\sqrt{N}}\sum_{j=0}^{N-1} e^{2\pi ijk/N}|j\rangle, \qquad \text{for } k = 0, 1, ..., N-1, \tag{16}$$

and form an orthonormal basis generated by the discrete Fourier transform F acting on the N-dimensional Hilbert space, i.e., $|u_k\rangle = F|k\rangle$, with

$$F = \frac{1}{\sqrt{N}}\sum_{j,m=0}^{N-1} e^{2\pi ijm/N}|j\rangle\langle m|. \tag{17}$$

Thus, there is a one by one correspondence between each orthonormal states $|u_k\rangle$ and one state from the computational basis $|k\rangle$. Moreover, the detection operators Π_k, defined in Equation (15), form a complete set in the N-dimensional Hilbert space,

$$\sum_{k=0}^{N-1}\Pi_k = \mathbf{1_N}. \tag{18}$$

In general, the success probability P_s for ME of N quantum states ρ_k, each prepared with *a priori* probability η_k, is given by [3,4]

$$P_s = \sum_{k=0}^{N-1}\eta_k tr(\Pi_k\rho_k). \tag{19}$$

For the case of N pure nonorthogonal equidistant states, $\rho_k = |\psi_k\rangle\langle\psi_k|$, prepared with equal *a priori* probabilities, $\eta_k = 1/N$, the optimum success probability simplifies to

$$P_s = |\langle u_0|\psi_0\rangle|^2, \tag{20}$$

as a consequence of the symmetry of the state set and the structure of the detectors operators $\Pi_k = |u_k\rangle\langle u_k|$, defined in Equation (15). The corresponding minimum error probability is then

$$P_e = 1 - P_s. \tag{21}$$

© 2025 by the author(s). Distributed under a Creative Commons CC BY license.

Preprints.org (www.preprints.org) | NOT PEER-REVIEWED | Posted: 25 June 2025 doi:10.20944/preprints202506.1981.v1

Therefore, the optimum success probability in ME of N pure nonorthogonal equidistant states with equal *a priori* probabilities, is given by

$$P_s = \frac{1}{N}\left(\sum_{k=0}^{N-1} C_k\right)^2, \tag{22}$$

where the coefficients C_k correspond to those of the fiducial state $|\psi_0\rangle$. The success probability given by Equation (22) is similar to that obtained for ME of N symmetric states prepare with equal *a priori* probability [17,39,40]. We notice here that using detectors operator different from $\Pi_k = |u_k\rangle\langle u_k|$ results in a higher probability of error. The worst case scenario occurs when the state is guessed randomly, which is equivalent to using the detectors operators of the form $\Pi'_k = |k\rangle\langle k|$, that is, performing a direct measurement of the equidistant states $|\psi_j\rangle$ in the computational basis $\{|k\rangle\}_{k=0}^{N-1}$. In such case, the success probability is $P_s = 1/N$, independently of the form of the states. A similar result is obtained even when using the optimum detector operators $\Pi_k = |u_k\rangle\langle u_k|$, if the inner product between the states satisfies $|S| = 1$. This corresponds to the situation in which all the states are identical, i.e., $|\psi_j\rangle = |0\rangle$ for $j = 0, 1, ..., N-1$. Since the states are completely indistinguishable in this scenario, the optimal success probability again reduces to $P_s = 1/N$.

Figure 3 shows the optimal success probability P_s, given by Equation (22), in the discrimination by ME of N equidistant states as a function of $|S|$, for several values of θ, and for: (a) $N = 3$, (b) $N = 7$ and (c) $N = 15$. When the states are orthogonal, $|S| = 0$, the maximum success probability $P_s = 1$ is achieved. This shows the well-known result that orthogonal states can be perfectly discriminated deterministically and without error. In all other cases, the discrimination involves some error, but this strategy minimizes the error probability. For any fixed value of N and θ, the success probability P_s decreases as $|S|$ increases, reaching its minimum value when the states become linearly dependent, that is, when $|S| = |S_\theta|$. On the other hand, if the number of states N and the modulus $|S|$ are fixed (within the allowed range), the success probability P_s decreases as the phase θ increases. This implies that it is more likely to correctly discriminate a set of linearly independent states than a set of linearly dependent ones. Moreover, as the number of states N increases, the only relevant case becomes $\theta = 0$. This is because, for $\theta \neq 0$, the allowed values of $|S|$ become increasingly close to zero, implying that the success probability under the ME strategy tends to one.

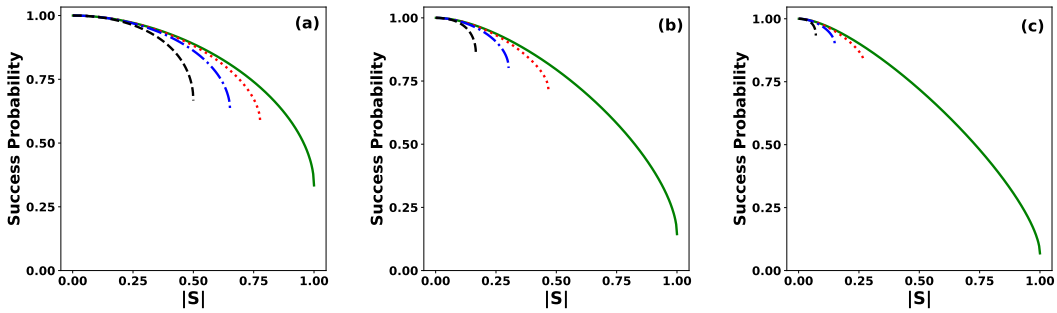

Figure 3. Success probability P_s for ME of equidistant states as a function of the modulus $|S|$ of the inner product, for the values: $\theta = 0$ (solid green line), $\theta = \pi/6$ (dotted red line), $\theta = \pi/3$ (dashed-dotted blue line), and $\theta = \pi$ (dashed black line), for: (a) $N = 3$, (b) $N = 7$, and (c) $N = 15$.

The ME strategy can be interpreted as a quantum communication scenario. On one side, Alice prepares and sends a quantum state $|\psi_j\rangle$, chosen from the set of equidistant states. On the other side, Bob located at a distant location, receives the state and applies quantum state discrimination to retrieve the classical information encoded in the state. To implement ME, Bob must first apply a unitary transformation to the received states that he received $|\psi_j\rangle$. For the set of equidistant states

© 2025 by the author(s). Distributed under a Creative Commons CC BY license.

Preprints.org (www.preprints.org) | NOT PEER-REVIEWED | Posted: 25 June 2025 doi:10.20944/preprints202506.1981.v1

considered here, the appropriate transformation is the discrete inverse Fourier transform F^{-1}. This operation transforms the equidistant states according to:

$$F^{-1}|\psi_j\rangle = \sum_{n=0}^{N-1} C_n \omega_n^j |u_{N-n}\rangle, \qquad \text{for } j = 0, 1, ..., N-1, \tag{23}$$

where

$$|u_{N-n}\rangle = \frac{1}{\sqrt{N}} \sum_{k=0}^{N-1} e^{-2\pi i k n/N} |k\rangle, \qquad \text{for } n = 0, 1, ..., N-1, \tag{24}$$

and thus, the evolution of the equidistant states under the F^{-1} transformation is given by

$$F^{-1}|\psi_j\rangle = \frac{e^{-2i\theta j/N}}{\sqrt{N}} \sum_{k,n=0}^{N-1} C_n e^{2\pi i n(j-k)/N} |k\rangle, \qquad \text{for } j = 0, 1, ..., N-1. \tag{25}$$

We assume that the subtraction $N - n$ in Equations (23) and (24) is performed modulo N. After applying the discrete inverse Fourier transform F^{-1}, Bob completes the ME by performing a projective measurement on the transformed states $|\hat{\psi}_j\rangle = F^{-1}|\psi_j\rangle$ in the computational basis $\{|k\rangle\}$. For instance, if Alice prepares and sends the state $|\psi_1\rangle$, Bob applies the transformation and obtains $|\hat{\psi}_1\rangle = F^{-1}|\psi_1\rangle$. He then performs a projective measurement in the basis $\{|k\rangle\}$, which yields one of N possible outcomes. If the outcome is $|1\rangle$, the state $|\psi_1\rangle$ has been correctly identified, and the discrimination is successful. The corresponding success probability is given by $P_s = |\langle 1|F^{-1}|\psi_1\rangle|^2 = |\langle 1|\hat{\psi}_1\rangle|^2$. Conversely, if the outcome is $|k\rangle$ with $k \neq 1$ an error occurs in the discrimination of $|\psi_1\rangle$. However, The ME strategy guarantees that this error occurs with the lowest possible probability among all quantum discrimination strategies.

A proposal for the experimental implementation of ME of $N = 4$ pure equidistant states is shown in Figure 4. This scheme is similar to previously reported setups for the discrimination of symmetric states [40,41]. The first stage corresponds to the state preparation. Alice prepares and sends one of the equidistant states, say $|\psi_1\rangle$. For this purpose, a single photon with horizontal polarization $|\rightarrow\rangle$ enters the experimental setup. Alice can prepare any of the equidistant states by adjusting the phases ω_k in each paths of propagation of the photon $|k\rangle$, and by setting the appropriate rotation angles in the polarizing beam splitters to generate the desired amplitudes C_k for each path. The prepared state then propagates through the channel. Upon receiving the state $|\psi_1\rangle$, Bob implements the inverse of the discrete Fourier transform F^{-1} in a four-dimensional Hilbert space. Finally, he performs a projective measurement in the computational basis $\{|k\rangle\}$. The initial single photon, after propagating through the discrimination setup, will be detected by one of the four detectors shown in Figure 4.

© 2025 by the author(s). Distributed under a Creative Commons CC BY license.

Preprints.org (www.preprints.org) | NOT PEER-REVIEWED | Posted: 25 June 2025 doi:10.20944/preprints202506.1981.v1

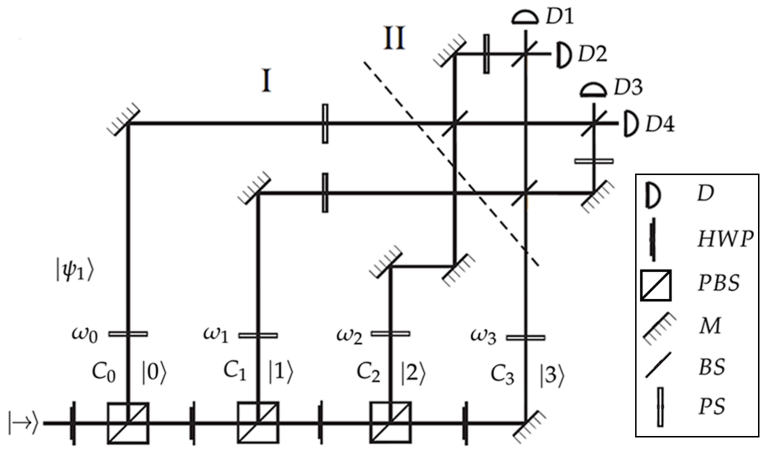

Figure 4. Experimental proposal for ME of four equidistant states: (I) State preparation: Alice send one of the equidistant states, e.g., $|\psi_1\rangle$, (II) Detection stage: Bob applies the inverse discrete Fourier transform F^{-1} in a four-dimensional Hilbert space and performs a projective measurement in the computational basis $\{|k\rangle\}$. HWP, half-wave plate; PBS, polarizing beam splitter; PS, phase shifter; BS, beam splitter; M, mirror; D, detector.

4. Quantum Coherence

As previously mentioned, in a quantum communication scenario, Alice prepares and sends to Bob one of the equidistant states $|\psi_j\rangle$, each with equal *a priori* probability $\eta_j = 1/N$. Bob aims to extract the encoded information by performing a quantum measurement on the received state. Therefore, the ensemble of possible states received by Bob is described by the density matrix ρ_B, which is given by

$$\rho_B = \frac{1}{N}\sum_{j=0}^{N-1} |\psi_j\rangle_B\langle\psi_j|. \tag{26}$$

Due to the symmetry of the equidistant states, this density matrix takes the simplified diagonal form

$$\rho_B = \sum_{k=0}^{N-1} C_k^2 |k\rangle_B\langle k|, \tag{27}$$

which is a diagonal state in the computational basis $\{|k\rangle_B\}$. Quantum coherence is associated with the ability of a quantum system to exhibit interference effects [42]. Such interference arises when the system's density matrix possesses non zero off-diagonal elements in a given basis. Accordingly, the state ρ_B, in Equation (27), exhibits no quantum coherence with respect to the basis $\{|k\rangle_B\}$, as it is diagonal in that basis. A canonical example of a maximally coherent state in a d-dimensional Hilbert space is given by [43,44]

$$|\psi\rangle = \frac{1}{\sqrt{d}}\sum_{k=0}^{d-1} |k\rangle, \tag{28}$$

which contains $\log_2 d$ bits of coherence, also referred to as cobit [43], relative to the computational basis $\{|k\rangle\}$. Quantum coherence has been formally established as a fundamental resource for the implementation of quantum protocols, and it is consumed during the execution of such protocols [43,45,46]. Several measures have been proposed to quantify quantum coherence, including the coherence cost, the relative entropy of coherence, and the ℓ_1 norm of coherence, among others [43]. To quantify the quantum coherence of the state ρ_B with respect to a given projective measurement Π, we employ the relative entropy of coherence [43,44], defined as

$$C(\rho_B, \Pi) = H(p_i) - S(\rho_B), \tag{29}$$

© 2025 by the author(s). Distributed under a Creative Commons CC BY license.

Preprints.org (www.preprints.org) | NOT PEER-REVIEWED | Posted: 25 June 2025 doi:10.20944/preprints202506.1981.v1

where, $H(p_i)$ is the Shannon entropy associated with the measurement outcome probabilities $\{p_i\}$, given by

$$H(p_i) = -\sum_{i=0}^{N-1} p_i \log_2 p_i, \tag{30}$$

and where

$$p_i = tr(\rho_B \Pi_i), \tag{31}$$

with $\Pi = \{\Pi_i\}_{i=0}^{N-1}$ being the projective measurement performed by Bob, and $S(\rho)$ is the von Neumann entropy, which is

$$S(\rho) = -\sum_{k=0}^{N-1} \lambda_k \log_2 \lambda_k, \tag{32}$$

where, λ_k are the eingenvalues of the density matrix ρ. For the set of equidistant states, the von Neumann entropy of ρ_B is given by

$$S(\rho_B) = -\sum_{k=0}^{N-1} C_k^2 \log_2 C_k^2, \tag{33}$$

which depends solely on the coefficients C_k and is independent of the quantum measurement Π applied by Bob. As shown in Equation (29), the quantum coherence depends both on the state ρ_B and on the quantum measurement Π, which, in this case, corresponds to ME. Then, the probability distribution $\{p_i\}$ is given by

$$p_i = tr(\rho_B \Pi_i) = \frac{1}{N}, \qquad \text{for } i = 0, 1, ..., N-1. \tag{34}$$

Therefore, the relative entropy of coherence when Bob implements ME is given by

$$C(\rho_B, \Pi) = \log_2 N + \sum_{k=0}^{N-1} C_k^2 \log_2 C_k^2, \tag{35}$$

which corresponds to the maximum coherence attainable from any projective measurement Π on the state ρ_B. This result holds because the Shannon entropy $H(p_i)$ reaches its maximum value, $H(p_i) = \log_2 N$, when the measurement is performed using the projectors Π_k defined in Equation (15). Thus, among all possible projective measurement, the ME strategy maximizes the quantum coherence of ρ_B.

Quantum coherence plays a fundamental operational role in the context of cryptographic randomness gain [47,48]. In particular, when an eavesdropper (Eve) is present in the communication channel, higher values of quantum coherence make it more difficult for her to extract information. For instance, if the set of quantum states is orthogonal, $|S| = 0$, the quantum coherence vanishes, and Eve can obtain complete information by performing a projective measurement without disturbing Bob's state ρ_B. At the opposite extreme, when all the states are identical, i.e., $|\psi_j\rangle = |0\rangle$, for all j, the state is pure, $\rho_B = |0\rangle_B\langle 0|$, and the quantum coherence reaches its maximum value of $\log_2 N$, where N the number of states in the ensamble. In this scenario, Eve cannot distinguish between the states and is left with no better strategy than randomly guessing the state sent by Alice. Figure 5 shows quantum coherence of ρ_B when is implemented ME of N pure equidistant states, as a function of $|S|$ for various values of the phase θ for: (a) $N = 3$, (b) $N = 7$, (c) $N = 15$. The behavior of quantum coherence $C(\rho_B, \Pi)$ differs notably from that of the success probability P_s. For any given values of θ and N, coherence reaches its minimum (zero) when the states are orthogonal $|S| = 0$, and its maximum ($\log_2 N$) when the states are linearly dependent with $|S_{\theta=0}| = 1$. For a fixed number of states N, within the allowed range of $|S|$, increasing the value of the phase θ from $\theta = 0$ to $\theta = \pi$ results in an increase in quantum coherence. This indicates that, for a given N, a more linearly dependent set of states exhibit greater coherence

© 2025 by the author(s). Distributed under a Creative Commons CC BY license.

Preprints.org (www.preprints.org) | NOT PEER-REVIEWED | Posted: 25 June 2025 doi:10.20944/preprints202506.1981.v1

than a linearly independent one. Furthermore, for any fixed $\theta \neq 0$, increasing the number of states N leads to a rapid decrease in coherence, which tends to zero as N becomes sufficiently large.

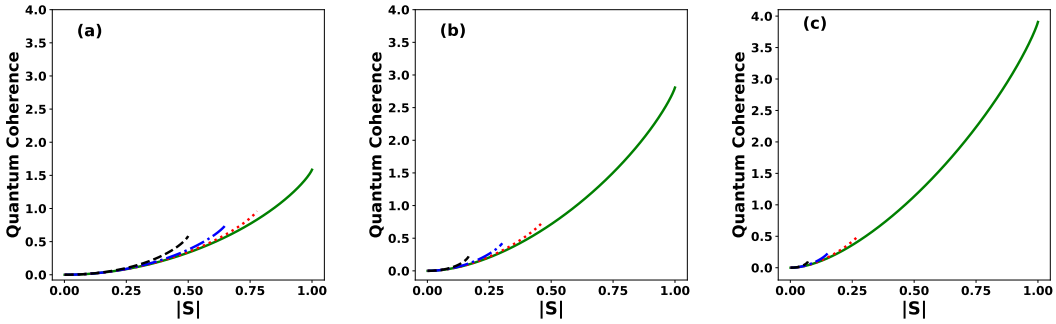

Figure 5. Quantum coherence of the initial state ρ_B, given in Equation (27), as a function of the modulus $|S|$ of the inner product, for different values of the phase: $\theta = 0$ (solid green line), $\theta = \pi/6$ (dotted red line), $\theta = \pi/3$ (dashed-dotted blue line), and $\theta = \pi$ (dashed black line) for: (a) $N = 3$, (b) $N = 7$ and (c) $N = 15$.

5. Channel Without Entanglement

In the ME scheme, Alice prepares a single copy of a quantum system in the state $|\psi_j\rangle$ and sends it to Bob with an *a priori* probability $\eta_j = 1/N$. We assume that, initially, Alice and Bob, share a separable quantum state ρ_{AB} of the form

$$\rho_{AB} = \frac{1}{N} \sum_{j=0}^{N-1} |j\rangle_A\langle j| \otimes |\psi_j\rangle_B\langle\psi_j|, \tag{36}$$

where $\{|j\rangle_A\}_{j=0}^{N-1}$ forms an orthonormal base for Alice's N-dimensional quantum system, and $\{|\psi_j\rangle_B\}_{j=0}^{N-1}$ are the pure equidistant states that Bob receives. Thereby, Alice and Bob share quantum and classical correlations encoded in the joint state ρ_{AB} defined in Equation (36). The initial state ρ_A of Alice's quantum system, that is, prior to the application of any transformation or measurement, is obtained by $\rho_A = \mathrm{tr_B}(\rho_{AB})$, where

$$\rho_A = \frac{1}{N} \sum_{j=0}^{N-1} |j\rangle_A\langle j|. \tag{37}$$

In a similar form, the initial state of Bob's quantum system can be obtained by tracing out Alice's subsystem from the global state, i.e., $\rho_B = \mathrm{tr_A}(\rho_{AB})$, where

$$\rho_B = \frac{1}{N} \sum_{j=0}^{N-1} |\psi_j\rangle_B\langle\psi_j|. \tag{38}$$

Once Bob receives a single copy of the quantum system prepared in one of the equidistant state $|\psi_j\rangle_B$, he implements the ME strategy. For that purpose, Bob first applies the unitary transformation F^{-1} to his quantum system, thereby transforming the global state ρ_{AB} into a new state $\hat{\rho}_{AB}$, given by

$$\hat{\rho}_{AB} = \frac{1}{N} \sum_{j=0}^{1} |j\rangle_A\langle j| \otimes |\hat{\psi}_j\rangle_B\langle\hat{\psi}_j|, \tag{39}$$

where $|\hat{\psi}_j\rangle_B = F^{-1}|\psi_j\rangle_B$. The unitary operation F^{-1}, defined in Equation (17) and applied by Bob, is a reversible process [49]. Therefore, it does not change the quantum correlations between Alice and Bob initially encoded in the global state ρ_{AB}. After this transformation, Bob performs a measurement on his subsystem, which yields N possible outcomes and, correspondingly, N conditional post-measurement

© 2025 by the author(s). Distributed under a Creative Commons CC BY license.

Preprints.org (www.preprints.org) | NOT PEER-REVIEWED | Posted: 25 June 2025 doi:10.20944/preprints202506.1981.v1

states $\rho^k_{A|B}$ for Alice's subsystem. Since Bob's measurement projects the state $|\hat{\psi}_j\rangle_B$ onto one the orthonormal basis states $|k\rangle_B$, the resulting conditional state for Alice is given by

$$\rho^k_{A|B} = \sum_{j=0}^{N-1} P_{kj}|j\rangle\langle j|, \qquad \text{for } k = 0, 1, ..., N-1, \tag{40}$$

where

$$P_{kj} = |\langle k|\hat{\psi}_j\rangle|^2 = |\langle u_k|\psi_j\rangle|^2 = \frac{1}{N}\left|\sum_{n=0}^{N-1} C_n\, e^{2\pi i(k-j)n/N}\right|^2, \tag{41}$$

with $P_{kk} = P_s = |\langle k|\hat{\psi}_k\rangle|^2$ is the success probability in ME for each $k = 0, 1, ..., N-1$. The final average joint state between Alice and Bob, denoted by ρ'_{AB}, after Bob performs his measurement in the basis $\{|k\rangle_B\}$, takes the following form:

$$\rho'_{AB} = \frac{1}{N}\sum_{k=0}^{N-1} \rho^k_{A|B} \otimes |k\rangle_B\langle k|. \tag{42}$$

Then, the final reduced states for Alice's and Bob's quantum subsystems are given by

$$\rho'_A = \frac{1}{N}\sum_{k=0}^{N-1} \rho^k_{A|B} = \frac{1}{N}\mathbf{1}_N, \tag{43}$$

$$\rho'_B = \frac{1}{N}\sum_{k=0}^{N-1} |k\rangle_B\langle k| = \frac{1}{N}\mathbf{1}_N. \tag{44}$$

Thereby, the final reduced state for Alice's subsystem remains unchanged, i.e., $\rho'_A = \rho_A$. It is convenient, using Equation (42) as follows:

$$\rho'_{AB} = \frac{1}{N}\sum_{k,j=0}^{N-1} P_{kj}|j\rangle_A\langle j| \otimes |k\rangle_B\langle k|. \tag{45}$$

From Equation (45), we can notice that, if Bob successfully discriminates the state $|\psi_j\rangle_B$, which is one of the states sent by Alice, the final shared state between Alice and Bob is $|j\rangle_A \otimes |j\rangle_B$, and this occurs with probability $P_{jj} = P_s$. Otherwise, if the discrimination attempt fails, the resulting state is $|j\rangle_A \otimes |k\rangle_B$ with $k \neq j$, indicating an error in identifying the state $|\psi_j\rangle$. Such an error occurs with the minimum error probability, given by $P_e = 1 - P_s$.

6. Classical Correlations and Quantum Discord

In a bipartite quantum state ρ_{AB}, the total amount of correlation, in the many copy scenario [50], is quantified by the quantum mutual information. This is defined as [50,51]

$$I(\rho_{AB}) = S(\rho_A) + S(\rho_B) - S(\rho_{AB}), \tag{46}$$

where $S(\rho)$ denotes the von Neumann entropy of the state ρ. In our ME scheme, we assume that Alice emits many independent and identically distributed (i.i.d.) copies of the bipartite state, i.e., $\sigma = \rho^n_{AB}$ for large n [52]. The entropy of the initial joint state ρ_{AB}, given by Equation (36), can be written as

$$S(\rho_{AB}) = S(\rho_A) + \frac{1}{N}\sum_{j=0}^{N-1} S(|\psi_j\rangle_B\langle\psi_j|) = S(\rho_A), \tag{47}$$

© 2025 by the author(s). Distributed under a Creative Commons CC BY license.

Preprints.org (www.preprints.org) | NOT PEER-REVIEWED | Posted: 25 June 2025 doi:10.20944/preprints202506.1981.v1

since each $|\psi_j\rangle_B$ is a pure state and therefore has zero entropy. Thus, the total correlation between Alice and Bob in the bipartite state ρ_{AB}, as defined in Equation (39), is given by the mutual information $I(\rho_{AB}) = S(\rho_B)$. Moreover, the quantum mutual information, $I(\rho_{AB})$, can be written as [51,53]

$$I(\rho_{AB}) = J(A|\{\Pi_B\}) + D(A|\{\Pi_B\}), \tag{48}$$

where, $J(A|\{\Pi_B\})$ denotes the classical correlations and $D(A|\{\Pi_B\})$ the quantum discord. Both quantities depend on the measurement implemented by Bob, represented by the set of projectors $\{\Pi_B\}$. However, their sum, the total mutual information, is independent of the choice of measurement [54], i.e., they are complementary to each other [14]. The classical correlations $J(A|\{\Pi_B\})$ between Alice and Bob are defined as [53,55]

$$J(A|\{\Pi_B\}) = S(\rho_A) - \frac{1}{N}\sum_{i=0}^{N-1} S(\rho^i_{A|b}), \tag{49}$$

which can be interpreted as the information about Alice's system that Bob gains through the measurement $\{\Pi_B\}$. In this work, we focus on quantifying the classical correlations between Alice and Bob, $J(A|\{\Pi_B\})$, when Bob implements the ME on the set of pure equidistant states. On the other hand, the problem of maximizing the classical correlation $J(A|\{\Pi_b\})$ over all possible measurements performed by Bob is a challenging task and is not addressed here. The maximal classical correlation

$$J(A|B) = \max_{\{\Pi_B\}} J(A|\{\Pi_B\}), \tag{50}$$

is known as the accessible information [9,10]. It corresponds to the classical mutual information maximized over all possible measurement strategies [12]. This optimization is generally difficult to perform and lies beyond the cope of the present work. Nevertheless, it is known that for $N = 2$, the quantum measurement that achieves the accessible information coincide with the one that minimizes the error probability in state discrimination [4,11]. Furthermore, for any N, the accessible information for a set of N pure, nonorthogonal equidistant states must be at least as large as the classical information obtained through the ME measurement. The classical correlations $J(A|\{\Pi_B\})$ in ME, given the symmetry, can be expressed as

$$J(A|\{\Pi_B\}) = S(\rho_A) - S(\rho^0_{A|B}), \tag{51}$$

where $S(\rho_A) = \log_2 N$, and the entropy of the conditional state $\rho^0_{A|B}$ is given by

$$S(\rho^0_{A|B}) = -\sum_{j=0}^{N-1} P_{0j}\log_2 P_{0j}, \tag{52}$$

with, P_{0j} defined in Equation (41). On the other hand, quantum discord $D(A|\{\Pi_B\})$, which quantifies the quantum correlations consumed or lost during the measurement process, is given by

$$D(A|\{\Pi_B\}) = S(\rho_B) - S(\rho_A) + S(\rho^0_{A|B}). \tag{53}$$

Figure 6 shows the classical correlation between Alice and Bob as a function of the modulus $|S|$ for: (a) $N = 3$, (b) $N = 7$ and (c) $N = 15$, and several values of the phase θ. The classical correlation reaches its maximum value when the equidistant states are orthogonal, i.e., $|S| = 0$. In this case, the maximum value is $\log_2 N$, indicating that Alice and Bob share total classical correlation. The corresponding final joint state is

$$\rho'_{AB} = \frac{1}{N}\sum_{j=0}^{N-1} |j\rangle_A\langle j| \otimes |j\rangle_B\langle j|. \tag{54}$$

© 2025 by the author(s). Distributed under a Creative Commons CC BY license.

Preprints.org (www.preprints.org) | NOT PEER-REVIEWED | Posted: 25 June 2025 doi:10.20944/preprints202506.1981.v1

As $|S|$ increases, the classical correlation $J(A|\{\Pi_B\})$ decreases, reaching its minimum value of zero when $|S| = 1$ and $\theta = 0$. This behavior arises because the initial joint state between Alice and Bob becomes a product state with no correlation, given by

$$\rho_{AB} = \left(\frac{1}{N} \sum_{j=0}^{N-1} |j\rangle_A \langle j| \right) \otimes |0\rangle_B \langle 0|. \tag{55}$$

For a fixed value of N and an allow value of $|S|$, increasing the phase θ from 0 to π leads to a decrease in the classical correlation. Moreover, we observe that larger values of N result in higher classical correlation between Alice and Bob. This highlights the importance of using a greater number of states in order to enhance the classical correlation, which is a desirable feature for the performance of the protocol.

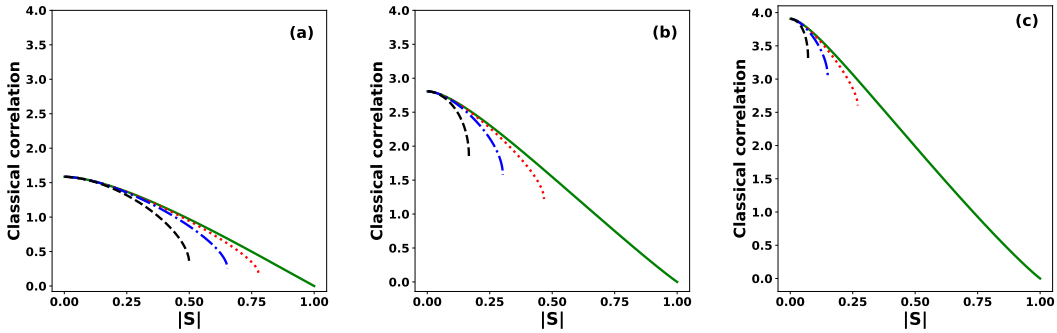

Figure 6. Classical correlation between Alice and Bob as a function of the modulus $|S|$ of the inner product, for different values of the phase: $\theta = 0$ (solid green line), $\theta = \pi/6$ (dotted red line), $\theta = \pi/3$ (dashed-dotted blue line), and $\theta = \pi$ (dashed black line), for: (a) $N = 3$, (b) $N = 7$ and (c) $N = 15$.

Figure 7 shows quantum coherence versus classical correlation between Alice and Bob for various values of the phase: $\theta = 0$ (solid green line), $\theta = \pi/6$ (dotted red line), $\theta = \pi/3$ (dashed-dotted blue line), and $\theta = \pi$ (dashed black line), for: (a) $N = 3$, (b) $N = 7$ and (c) $N = 15$. We observe that both quantities, quantum coherence and classical correlations, lie within the same range, namely $[0, \log_2 N]$. It is important to highlight here the operational interpretation of the quantum coherence as a quantifier of cryptographic randomness gain [47,48]. Therefore, for a secure and efficient protocol, we expect that Alice and Bob share a significant amount of classical correlation while maintaining sufficiently high quantum coherence. For example, when the set of states is orthogonal $|S| = 0$ the initial joint state takes the form $\rho_{AB} = \frac{1}{N} \sum_j |j\rangle_A \langle j| \otimes |u_j\rangle_B \langle u_j|$, which exhibits maximal classical correlation of $\log_2 N$ bit but zero quantum coherence. In contrast, when the set of states is identical $|S| = 1$, the initial joint state becomes $\rho_{AB} = (\frac{1}{N} \sum_j |j\rangle_A \langle j|) \otimes |0\rangle_B \langle 0|$, a product state with no classical correlation but exhibiting maximal quantum coherence, equivalent to $\log_2 N$ bits of randomness. Hence, Alice and Bob should choose an initial joint state ρ_{AB} that simultaneously exhibits high classical correlation and high quantum coherence. This trade-off can be optimally achieved when the phase of the inner product is $\theta = 0$ and the number of states N is large.

© 2025 by the author(s). Distributed under a Creative Commons CC BY license.

Preprints.org (www.preprints.org) | NOT PEER-REVIEWED | Posted: 25 June 2025 doi:10.20944/preprints202506.1981.v1

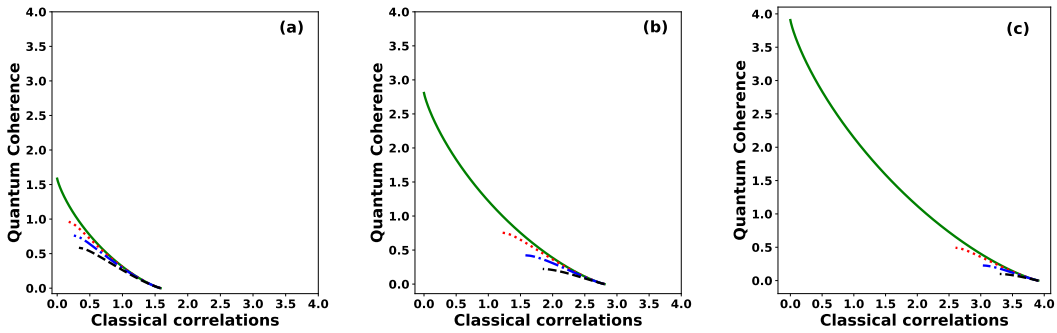

Figure 7. Quantum coherence versus classical correlation between Alice and Bob for different values of the phase: $\theta = 0$ (solid green line), $\theta = \pi/6$ (dotted red line), $\theta = \pi/3$ (dashed-dotted blue line), and $\theta = \pi$ (dashed black line), for: (a) $N = 3$, (b) $N = 7$ and (c) $N = 15$.

7. Conclusions

We have studied the problem of minimum error discrimination for a set of N pure, nonorthogonal equidistant states, each prepared with equal *a priori* probability. The equidistant states resemble symmetric states but are uniquely characterized by a single complex parameter, which is the inner product S between any pair of the equidistant states. This feature allows for a detailed analysis of any quantity of interest as a function of the number of states in the set N, the modulus $|S|$, and the phase θ of the inner product. In this work, we described the behavior of the success probability, quantum coherence, and classical correlations under the minimum error strategy in terms of these parameters. We also proposed an experimental scheme for implementing minimum error discrimination of equidistant states. As an application, we present a quantum communication protocol in which Alice prepares and sends an equidistant state to Bob, who then applies the ME to extract the encoded classical information. This framework allows us to quantify the classical information shared between Alice and Bob through the ME process. Moreover, we determine the quantum coherence involved in Bob's implementation of the ME, interpreting it as the gain of cryptographic randomness. Interestingly, our findings reveal a trade-off: greater classical information sharing between Alice and Bob corresponds to lower randomness generation in the protocol, and vice versa. Future work will focus on determining the accessible information, i.e., the maximal classical correlation achievable over all possible measurements, for the set of equidistant states. Although this quantity remains unknown, it must be no less than the classical information obtained under the ME. Moreover, in the special case of two pure nonorthogonal states, it is well established that the measurement that allows the extraction of the accessible information coincides with the minimum error measurement.

Author Contributions: O.J. provided the idea of the study, did the calculations of the study and performed critical revision of the manuscript.

Funding: This work was supported by an internal grant Universidad Mayor PUENTE-2024-17.

Conflicts of Interest: "The author declare no conflicts of interest."

References

1. Gisin, N.; Thew, R. Quantum communication.*Nature Photon* (**2007**), 1, 165-171. [CrossRef]
2. Vallone, G.; Bacco, D.; Dequal, D.; Gaiarin, S.; Luceri, V.; Bianco, G.; Villoresi, P. Experimental Satellite Quantum Communications. *Phys. Rev. Lett.* **2015**, 115, 040502. [CrossRef]
3. Bergou, J.; Hillery, M. *Introduction to the Theory of Quantum Information Processing*, Springer Science + Business Media: New Yprk, NY, USA, 2013.
4. Barnett, S.M.; Croke, S. Quantum State Discrimination. *Adv. Opt. Photon.* **2009**, 1, 238-278. [CrossRef]
5. Bennett, C.H.; Brassard, G. Quantum Cryptography: Public Key Distribution and Coin Tossing. *Theoretical Computer Science* (**1984**) 560:175-179.
6. Holevo, A. S. Statistical Decision Theory for Quantum Systems. *J. Multivariate Anal.* **1973**, 3, 337-394.

© 2025 by the author(s). Distributed under a Creative Commons CC BY license.

Preprints.org (www.preprints.org) | NOT PEER-REVIEWED | Posted: 25 June 2025 doi:10.20944/preprints202506.1981.v1

7. Yuen, H. P.; Kennedy, R. S.; Lax, M. Optimum testing of multiple hypothesis in quantum detection theory. IEEE Transactions on Information Theory **1975**, 21, 125.
8. Helstrom, C. W. *Quantum Detection and Estimation Theory*, Academic Press, 1976.
9. Dall'Arno, M.; D'Ariano, G. M.; Sacchi, M.F. Informational power of quantum measurements. *Phys. Rev. A* **2011**, 83, 062304. [CrossRef]
10. Sasaki, M.; Barnett, S.; Jozsa, R.; Osaki, M.; Hirota, O. Accessible information and optimal strategies for real symmetrical quantum sources. *Phys. Rev. A* **1999**, 59, 3325. [CrossRef]
11. Levitin, L.B. *Optimal quantum measurements for two pure and mixed states*. In *Quantum Communications and Measurement*, Belavkin, V.P., Hirota, O., Hudson, R.L. Eds.; Plenum: New York, NY, USA, 1995;pp.439-448.
12. Clarke, R. B. M.; Kendon, V. M.; Chefles, A.; Barnett, S. M.; Riis, E.; Sasaki, M. Experimental realization of optimal detection strategies for overcomplete states. *Phys. Rev. A* **2001**, 64, 012303. [CrossRef]
13. Nakahira, K.;Kato,K; Usuda,T.S. Generalized quantum state discrimination problems. *Phys. Rev. A* **2015**, 91, 052304. [CrossRef]
14. Jiménez, O; Solís-Prosser, M.A.; Neves, L.; Delgado, A. Quantum Discord, Thermal Discord, and Entropy Generation in the Minimum Error Discrimination Strategy, Entropy (**2019**), 21, 263. [CrossRef]
15. Jiménez, O; Solís-Prosser, M.A.; Neves, L.; Delgado, A. Mutual Information and Quantum Discord in Quantum State Discrimination with a Fixed Rate of Inconclusive Outcomes, Entropy (**2021**), 23, 73. [CrossRef]
16. Suzuki, J.; Assad S.M.; Englert, B. Accessible information about quantum states: An open optimization problem. Mathematics of Quantum Computation and Quantum Technology, 1st Edition, 2007, Chapman and Hall/CRC.
17. Ban, M.; Kurokawa, K.; Momose, Rei, Hirota, O. Optimun Measurements for Discrimination Among Symmetric Quantum States and Parameter Estimation. International Journal of Theoretical Physics, Vol.36, No. 6, 1997.
18. Barnett, S. Minimum-error discrimination between multiply symmetric states. *Phys. Rev. A*, **2001**, 64, 030303(R). [CrossRef]
19. Chou, C.L.; Hsu, L.Y. Minimum-error discrimination between symmetric mixed quantum states. *Phys. Rev. A*, **2003**, 68, 042305. [CrossRef]
20. Jafarizadeh, M.A.; Sufiani, R.; Khiavi, Y.M. Minimum error discrimination between similarity-transformed quantum states. *Phys. Rev. A*, **2011**, 84, 012102. [CrossRef]
21. Bae, J. Structure of minimum-error quantum state discrimination. *New J. Phys.* (**2013**) 15, 073037. [CrossRef]
22. Varga, A.; Adam, P.; Bergou, J. A. Maximum information measurement for qubit states. Scientifec Reports (**2024**), 14, 11888. [CrossRef]
23. Shor, P. On the number of elements needed in a POVM attaining the accessible information (**2000**) quant-ph/0009077.
24. Oreshkov, O.; Calsamiglia, J.; Muñoz-Tapia, R.; Bagan, E. Optimal signal states for quantum detectors. *New J. Phys.* (**2011**) 13, 073032. [CrossRef]
25. Ban, M.; Osaki, M.; Hirota, O. Upper bound of the accessible information and lower bound of the Bayes cost in quantum signal-detection processes. *Phys. Rev. A*, **1996**, 54, 2718. [CrossRef]
26. Fuchs, C. A.; Caves, C.M. Ensamble-Dependent Bounds for Accessible Information in Quantum Mechanics. *Phys. Rev. Lett.*, **1994**, 73, 3047. [CrossRef]
27. Roa, L.; Delgado A.; Fuentes-Guridi, I. Optimal conclusive teleportation of quantum states. *Phys. Rev. A*, **2003**, 68, 022310. [CrossRef]
28. Neves, L.; Solís-Prosser, M. A.; Delgado, A.; Jiménez O. Quantum teleportation via maximum-confidence quantum measurements. *Phys. Rev. A*, **2012**, 85, 062322. [CrossRef]
29. Delgado, A.; Roa, L.; Retamal, J. C.; Saavedra, C. Entanglement swapping via quantum state discrimination. *Phys. Rev. A* **2005**, 71, 012303. [CrossRef]
30. Solís-Prosser, M. A.; Delgado, A.; Jiménez, O.; Neves, L. Deterministic and probabilistic entanglement swapping of nonmaximally entangled states assisted by optimal quantum state discrimination. *Phys. Rev. A* **2014**, 89, 012337. [CrossRef]
31. Phoenix, S. J. D.; Barnett, S. M.; Chefles, A. Three-state quantum cryptography. *J. Mod. Opt.***2000**, 47, 507. [CrossRef]
32. Pati, A. K.; Parashar, P.; Agrawal, P. Probabilistic superdense coding. *Phys. Rev. A* **2005**, 72, 012329. [CrossRef]
33. Barnett, S. M.; Riis, E. Experimental demonstration of polarization discrimination at the Helstrom bound. *J. Mod. Opt.* **1997**, 44, 1061. [CrossRef]

© 2025 by the author(s). Distributed under a Creative Commons CC BY license.

Preprints.org (www.preprints.org) | NOT PEER-REVIEWED | Posted: 25 June 2025 doi:10.20944/preprints202506.1981.v1

34. Waldherr, G.; Dada, A. C.; Neumann, P.; Jelezko, F.; Andersson, E.; Wrachtrup, J. Distinguishing between Nonorthogonal Quantum States of a Single Nuclear Spin. *Phys. Rev. Lett.* **2012**, 109, 180501. [CrossRef]
35. Solís-Prosser, M.A.; Fernandes, M.F.; Jiménez, O.; Delgado A.; Neves, L. Experimental Minimum-Error Quantum-State Discrimination in High Dimensions. *Phys. Rev. Lett.* **2017**, 118, 100501. [CrossRef]
36. Roa, L.; Hermann-Avigliano, C.; Salazar, R.; Klimov, A. B. Conclusive discrimination among N equidistant pure states. *Phys. Rev. A* **2011**, *84*, 014302.
37. Paiva-Sánchez, C.; Burgos-Inostroza, E.; Jiménez, O.; Delgado, A. Quantum tomography via equidistant states. *Phys. Rev. A* **2010**, *82*, 032115.
38. Jiménez, O.; Roa, L.; Delgado, A. Probabilistic cloning of equidistant states. *Phys. Rev. A* **2010**, *82*, 022328.
39. Raynal, P.; Lütkenhaus, N.; Van Enk, S.J. Reduction theorems for optimal unambiguous state discrimination of density matrices. *Phys. Rev. A* **2003**, 68, 022308. [CrossRef]
40. Jiménez, O.; Sánchez-Lozano, X.; Burgos-Inostroza, E.; Delgado, A., Saavedra, C. Experimental scheme for unambiguous discrimination of linearly independent symmetric states. *Phys. Rev. A.* **2007**, 76, 062107. [CrossRef]
41. Solís-Prosser, M.A.; Delgado, A.; Jiménez, O.; Neves, L. Parametric separation of symmetric pure quantum states. *Phys. Rev. A* (2016) 93, 012337. [CrossRef]
42. Bromley, T.R.; Cianciaruso, M.; Adesso, G. Frozen Quantum Coherence. *Phys. Rev. Lett.* (2015) 114, 210401. [CrossRef]
43. Streltsov, A.; Adesso, G.; Plenio, M.B. Colloquium: Quantum coherence as a resource. *Rev. Mod. Phys.* **2017**, 89, 041003. [CrossRef]
44. Baumgratz, T.; Cramer, M.; Plenio, M.B. Quantifying Coherence. *Phys. Rev. Lett.* (2014) 113, 140401. [CrossRef]
45. Jiménez, O.; Solís-Prosser, M.A.; Delgado, A.; Neves, L. Quantum resources for assisted optimal state discrimination. *Phys. Rev. Research* **2024**, 6, 043303. [CrossRef]
46. Melo, L.F.; Jiménez, O.; Neves, L. Coherence based on positive operator-valued measures for standard and concatenated quantum state discrimination with inconclusive results. *Phys. Rev. A* **2025**, 111, 012403. [CrossRef]
47. Yuan, X.; Zhou, H.; Cao, Z.; Ma, X. Intrinsic randomness as a measure of quantum coherence. *Phys. Rev. A.* **2015**, 92, 022124. [CrossRef]
48. Bischof, F.; Kampermann, H.; Bruß, D. Quantifying coherence with respect to general quantum measurements. *Phys. Rev. A.* **2021**, 103, 032429. [CrossRef]
49. Horodecki, M.; Horodecki, P.; Horodecki, R.; Oppenheim, J.; Sen(De), A.; Sen U.; Synak-Radtke, B. Local versus nonlocal information in quantum-information theory: Formalism and phenomena. *Phys. Rev. A* **2005**, 71, 062307. [CrossRef]
50. Groisman, B.; Popescu S.; Winter A. Quantum, classical, and total amount of correlations in a quantum state. *Phys. Rev. A* **2005**, 72, 032317. [CrossRef]
51. Ollivier, H.; Zurek, W.H. Quantum Discord: A Measure of the Quantumness of Correlations. *Phys. Rev. Lett.* **2001**, 88, 017901. [CrossRef]
52. Dahlsten, O.; Renner, R.; Rieper, E.; Vedral, V. Inadequacy of von Neumann entropy for characterizing extractable work. *New J. Phys.* **2011**, 13, 053015. [CrossRef]
53. Modi, K.; Brodutch, A.; Cable, H.; Paterek, T.; Vedral, V. The classical-quantum boundary for correlations: Discord and related measures. *Rev. Mod. Phys.* **2012**, 84, 1655. [CrossRef]
54. Zwolak, M.; Zurek, W.H. Complementarity of quantum discord and classically accessible information. *Sci. Rep.* **2013**, 3,1729. [CrossRef]
55. Herderson, L.; Vedral, V. Classical, quantum and total correlations. *J. Phys. A: Math. Gen.* **2001**, 34, 6899. [CrossRef]

Disclaimer/Publisher's Note: The statements, opinions and data contained in all publications are solely those of the individual author(s) and contributor(s) and not of MDPI and/or the editor(s). MDPI and/or the editor(s) disclaim responsibility for any injury to people or property resulting from any ideas, methods, instructions or products referred to in the content.

© 2025 by the author(s). Distributed under a Creative Commons CC BY license.